Available online at www.sciencedirect.com
SCIENCE DIRECT®
Chemical Physics Letters 390 (2004) 285–289
CHEMICAL PHYSICS LETTERS
www.elsevier.com/locate/cplett

Reversibly strain-tunable elastomeric photonic crystals

Jian Li, Yang Wu, Jun Fu, Yang Cong, Juan Peng, Yanchun Han *

State Key Laboratory of Polymer Physics and Chemistry, Changchun Institute of Applied Chemistry, Chinese Academy of Sciences, 5625 Renmin Street, Changchun 130022, PR China

Received 23 November 2003; in final form 2 April 2004
Available online 30 April 2004

Abstract

Reversibly strain-tunable polymeric photonic crystals made of thermoplastic polyester elastomer (TPEE) were fabricated by using the self-assembled silica opals as templates. The stop band of the polymeric photonic crystal locates at the near infrared (IR) regime in its transmission spectrum, and exhibits a blue shift with the increase of the incident angle. Because of the elasticity of the TPEE, the stop band of the TPEE photonic crystal can also be reversibly tuned at ambient temperature through to and fro uniaxially or biaxially stretching and recovering by changing the lattice spacing and the symmetry of the crystal along (1 1 1) plane.

1. Introduction

Photonic bandgap (PBG) materials have recently generated great interests due to their potential applications in photonics, such as low-loss waveguides, optical cavities, zero threshold microlasers, light-emitting diodes, optical switches, and tunable filters [1–6]. However, the realization of photonic crystals for optical or near infrared (IR) frequencies is still a major technological challenge. Many techniques have been developed to fabricate PBG materials, including conventional microlithographic techniques [7], laser-guided stereolithography [8], two-photon induced deposition or polymerization [9], and self-assembly of phase-separating block co-polymers [10], colloidal crystals [11,12], and inverse-opal techniques [13–15].

Because they can be used to create large-area, low-cost, and flexible devices, polymeric PBG materials have attracted much attention in recent years. Thomas and co-workers [10] reported their work in making photonic crystals through phase separation of block copolymers. And polymeric photonic crystals also have been fabricated from PMMA, polyurethane, epoxy resins, etc by colloidal templating [16–18]. For many applications it is advantageous that the photonic bandstructure is tunable. Since polymers are flexible and can be deformed fairly easily, the crystal lattice of the polymeric photonic crystals can be changed [19–28]. In other words, the photonic bandgap can be shifted with the change of the symmetry of the crystal lattice. A two-dimensional strain-tunable photonic band gap crystal has been reported, whose bandgap can be tuned by distorting the symmetry of the crystal from a regular hexagonal to a quasihexagonal lattice by means of field driven strain using a piezoelectric material [19]. Polymerized colloidal crystal hydrogel films were also used to fabricate tunable photonic materials, which can be applied in sensing [20–28]. In this work, three dimensional (3D) polymeric photonic crystals, which can be reversibly tuned at room temperature by to and fro uniaxially or biaxially stretching the crystal and recovering along the (1 1 1) plane, were fabricated from thermoplastic polyester elastomer (TPEE) by colloidal templating methods. The stop band of the polymeric photonic crystal is at the near IR regime in its transmission spectrum.

* Corresponding author. Fax: +86-431-526-2126.
E-mail addresses: jianli@ciac.jl.cn (J. Li), ychan@ciac.jl.cn (Y. Han).

0009-2614/$ - see front matter © 2004 Elsevier B.V. All rights reserved.
doi:10.1016/j.cplett.2004.04.028

2. Experimental

In our experiment, monodispersed silica microspheres with a diameter of ~700 nm were purchased as an aqueous suspension from Bangs Laboratories, Ins. Silica opals were self-organized by sedimentation of the suspension of the silica beads under ultrasonic in a polymer cell on a flat silicon wafer at about 40 °C for 3–4 h. Opals composed of silica spheres were sintered by heat treatment in air (drying at 130–150 °C followed by thermal annealing at 950 °C for 3 h) [29]. A 2 wt% TPEE solution in dichloromethane was infiltrated into the annealed silica opal template. After drying under vacuum at 50 °C for 8 h, the silica opal template was etched with a 5 wt% HF aqueous solution for 18 h. The HF solution was wicked away with deionized water and the sample was dried under vacuum at 50 °C for 5 h, and a polymeric inverse opal was obtained.

Scanning electron microscopy (SEM) micrographs were taken using a JOEL JXA-840 microscope and a Philips XL-30-ESEM-FEG instrument operating at 20 kV. Optical transmission spectra of photonic materials were measured on a JASCO V-570 UV–VIS–NIR spectrophotometer to probe the existence of stop bands.

3. Results and discussion

The SEM micrograph in Fig. 1a shows the pattern of the silica opal template. The Fast Fourier transforms of the pattern (inset) indicate that the opal template has a three-dimensional long-range periodic structure, and the units are the face-centred cubic (fcc) close-packed cells. The (1 1 1) face is parallel to the silicon substrate. By annealing at 950 °C, the necks between the spheres formed and the mechanical properties of the opals increased (Fig. 1b). It is necessary in the later stage when the silica template is removed. The necks connecting the silica spheres act as channels through which the etchant flows. The good connectivity provided by the sintering allows the etchant to reach the whole sample to fully remove the silica matrix. As a result of being sintered, the silica beads shrink and have a diameter of 606 nm.

After the silica opal template was prepared, a TPEE solution of dichloromethane was allowed to infiltrate into the network of the channels between microspheres by capillary action. After drying, the template of silica opals was completely removed from the composite system by etching with an HF aqueous solution. As shown in Fig. 1c, the removal of the colloidal spheres results in a 3D porous structure that has a highly ordered archi-

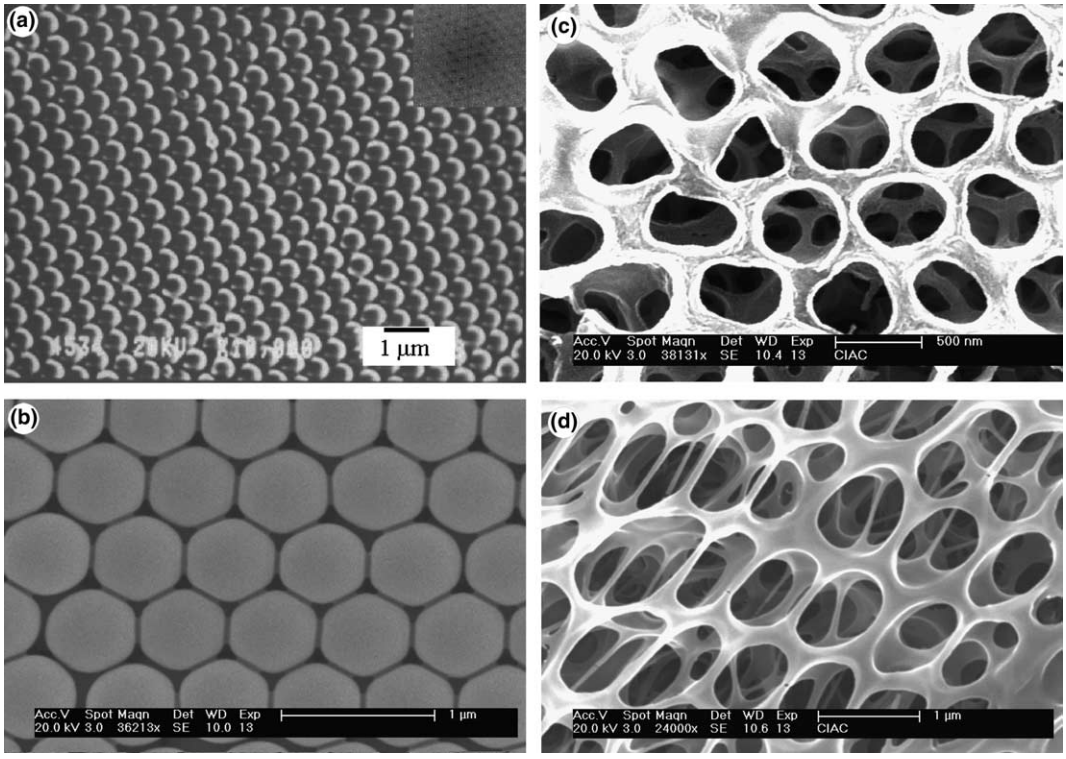

Fig. 1. (a) SEM image of a (1 1 1) facet from a crystalline assembly of 700 nm silica beads. The inset shows two-dimensional Fast Fourier transforms (FFT) of topography, illustrating the long-range order and registry of the crystal. (b) SEM image of the silica colloidal crystal sintered at 950 °C. (c) SEM image of TPEE inverse opals at the stretch-free state, exhibiting the perfection of the replication process. (d) SEM image of TPEE inverse opals after being stretched.

tecture of uniform air spheres interconnected to each other by small circular 'windows'. The porous materials are named polymeric inverse opals that have an open, periodic 3D framework packed into a hexagonal array, which is complementary to that of an opaline structure. Fig. 1d is a SEM image of a TPEE inverse opal film, which had been stretched along the (1 1 1) plane. The retentively excellent 3D ordered structure of the stretched inverse opal indicates that the strain did not spoil the quality of the inverse opal. Such ordered periodic modulation of dielectric constant between the polymer and the air gives rise to interesting optical properties, including the presence of stop bands.

At the different stages of the inverse opal fabrication, the diffractive optical properties of these 3D arrays have been characterized by their transmission spectra. Transmission experiments were performed at different incident angles along the (1 1 1) direction of the fcc lattice. As shown in Fig. 2, silica opals and polymeric inverse opals do not provide a complete photonic bandgap, but they give a stop band in the transmission spectra, respectively. The silica opal exhibits a stop band at a wavelength of about 1401 nm when the incident light is normal to the sample surface (shown in Fig. 2a). The spectra of silica opals exhibit a blue shift of the peak wavelength of the stop band when the angle of incidence varies from 0° to 40° with respect to the surface normal. With the increase of the incident angle, the transmission peak gradually descends.

Fig. 2b shows the absorption spectra of a composite system made of the silica opal and the polymer. A stop band at around 1450 nm was observed, which has a red shift compared to that of the silica opal. After the silica opal template was removed, the polymeric inverse opal, as a replica of silica opal, also exhibits a stop band at a wavelength of 1101 nm (Fig. 2c). Similar to the silica opal, the transmission peak of the polymeric inverse opal shifts to a shorter wavelength when the incident angle increases. The optical properties of these systems are dominated by strong diffraction effect, which can be described by the Bragg's law,

$$\lambda = 2\bar{n}d\sqrt{1 - \frac{1}{\bar{n}^2}\sin^2\theta}, \tag{1}$$

where d is the spacing between crystalline planes in the (1 1 1) direction. In the case of the polymeric inverse opal, this spacing is related to the air spheric diameter D by $d = \sqrt{2/3}D$ for the fcc structure. θ is the incident angle with respect to the surface normal. And $\bar{n}$, the average refractive index, can be approximated by the equation:

$$\bar{n} = \sqrt{f_P n_P^2 + f_{air} n_{air}^2}. \tag{2}$$

Here, f_P and f_{air} are the filling fractions for the polymer and the air spheres, respectively. The refractive index of TPEE is 1.54 and that of silica colloidal crystals is 1.45.

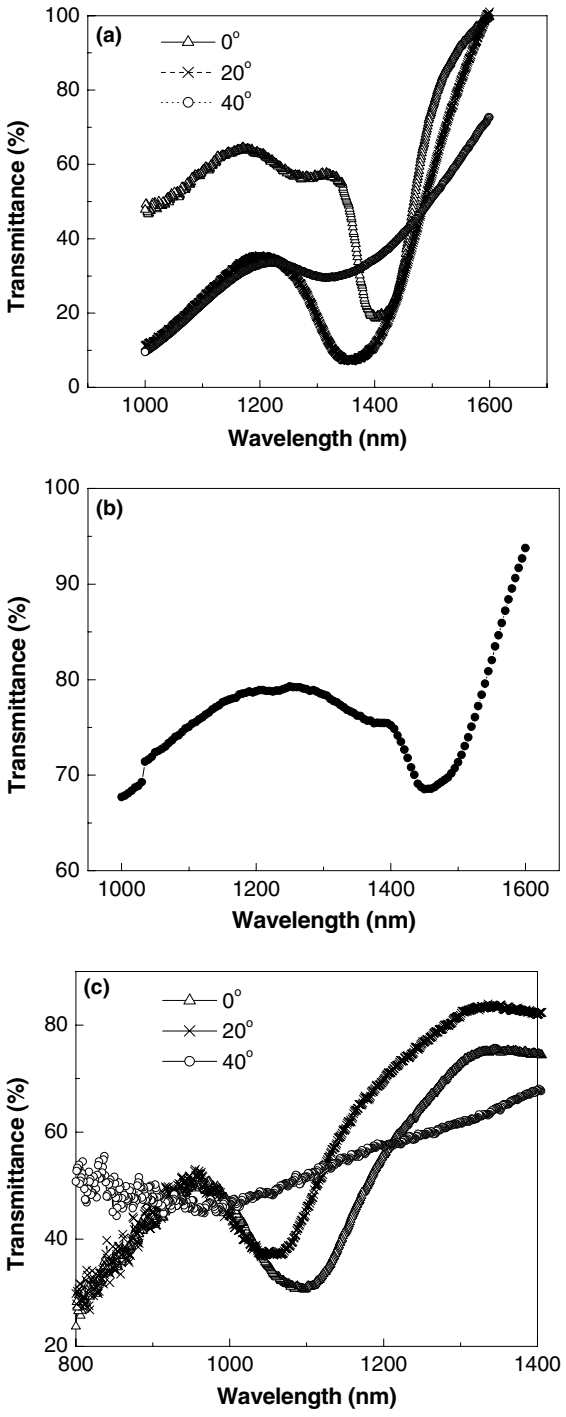

Fig. 2. Optical transmission spectra curves for different incidence angles, θ with respect to the surface normal of the different stage samples: (a) from the silica opal; (b) from the composite system made of the silica opal and the TPEE; (c) from the TPEE inverse opal before being deformed.

The TPEE inverse opal, as an excellent replica of the silica colloidal crystal, has a center-to-center distance of about 606 nm between the neighboring air spheres. According to Bragg's law, the filling fractions are calculated to be $f_p = 0.165$ and $f_{air} = 0.835$ by the

transmission spectrum of the composite system, which fit the transmission spectrum of the TPEE inverse opal in Fig. 2c. Compared to that of the silica opal, the stop band of the polymeric inverse opal exhibits a blue shift. The blue shift results from the decrease of the average refractive index of the polymeric inverse opal with respect to that of the silica opal.

According to the Bragg's law, the stop band may be tuned by changing the distance between crystalline planes in the (1 1 1) direction as well. The lattice spacing of the elastomeric photonic crystal can be altered through distorting the symmetry of the crystal from a regular fcc to a quasi fcc lattice by means of uniaxially or biaxially stretching the PBG material. This breaking of the fcc symmetry may be useful for shifting the diffraction and creating unique PBG materials. The optical properties of a TPEE photonic crystal in different states are shown in Fig. 3. Fig. 3a presents the transmission spectra of a PBG film at normal incidence in the stretch-free state and under various strain loadings, respectively. In the original stretch-free state, the stop band locates at 1101 nm. Upon applying a uniaxial strain of 0.04 and 0.13 at ambient temperature, however, the stop band shifts down to a wavelength of 1091 and 1086 nm, respectively. When subjected to a biaxial stretch, a greater stop-band blue shift is observed. For example, the stop band shifts to 1046 nm when the material is stretched biaxially ($\varepsilon_x = 0.17$, $\varepsilon_y = 0.14$). The stop band shifts can be attributed to the decrease of the $d_{1\,1\,1}$ interplanar spacings by stretching the crystal along the (1 1 1) plane. In Fig. 3b, the shift of the stop band as a function of the stretch ratio is shown. With additional strain, 80 nm or greater of band shifts can be attained. Unfortunately, with the increase of the stretch ratio, the peak becomes broader and less well defined due to the increase of disorder in the array [30]. Moreover, due to the elasticity of the polymer, the release of the strain on the stretched sample results in an immediate recovery of the band gap position within 2–3 nm of the initial stretch-free state. As shown in Fig. 3a, the stop band of a TPEE photonic crystal in the unloaded state locates at 1098 nm, which is within 3 nm of that of the original stretch-free state. This indicates that the stop band of the TPEE photonic crystal can reversibly tuned with a high response speed by to and fro stretching the elastomeric sample and recovering.

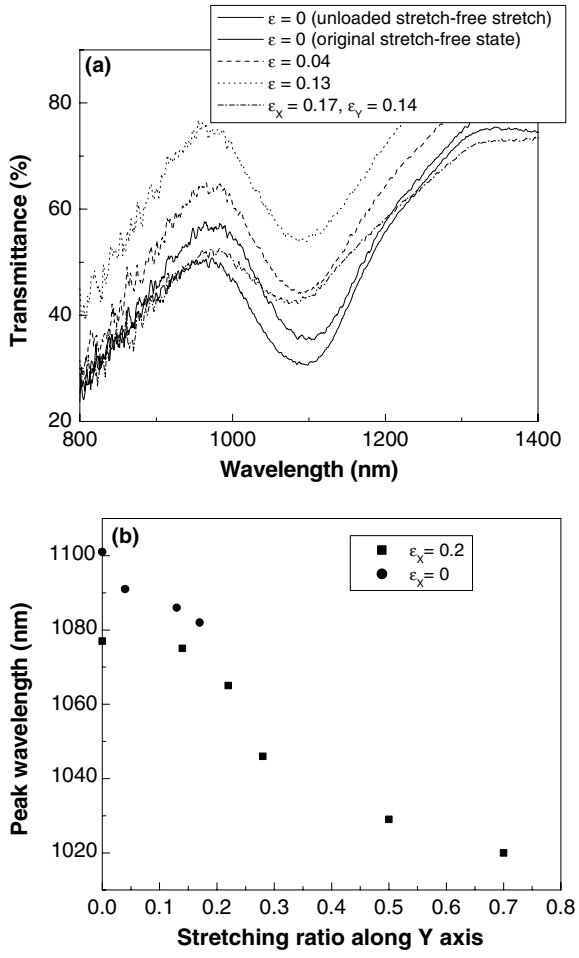

Fig. 3. (a) Optical transmission spectra curves of TPEE inverse opals for original stretch-free state (thick solid line), unloaded stretch-free state (thin solid line), uniaxial stretch (dash or dot line), and biaxial stretch (dash dot line). (b) Peak wavelength of the stop-band as a function of stretch ratio (ε_y) in Y axis along (1 1 1) plane: $\varepsilon_x = 0$ (●), $\varepsilon_x = 0.2$ (■).

4. Conclusions

In summary, we present the synthesis and characterization of a mechanically robust, optically tunable TPEE inverse opal with well-defined pore structure by using silica opal template. The inverse opals produced can be used as PBG materials. The stop bands of TPEE photonic crystals can be reversibly tuned through changing the angle of incidence or distorting the symmetry of the crystal.

Acknowledgements

This work is subsidized by the National Natural Science Foundation of China (59825113, 50125311, 20074037, 50373044, 20334010, 20274050, 50390090, 50373041), the Ministry of Science and Technology of China (2003CB615600, 2002CCAD4000), and the Chinese Academy of Sciences (Distinguished Talents Program, KJCX2-SW-H07, KGCX2-205-03).

References

[1] E. Yablonovitch, Phys. Rev. Lett. 58 (1987) 2059.
[2] S. John, Phys. Rev. Lett. 58 (1987) 2486.

[3] J.D. Joannopoulos, R.D. Meade, J.N. Winn, Photonic Crystals: Molding the Flow of Light, Princeton University Press, Princeton, NJ, 1995.
[4] J.D. Joannopoulos, P.R. Villeneuve, S. Fan, Nature 387 (1997) 830.
[5] B. Temelkuran, E. Ozbay, Appl. Phys. Lett. 74 (1999) 486.
[6] O. Painter, R.K. Lee, A. Scherer, A. Yariv, J.D. O'Brien, P.D. Dapkus, I. Kim, Science 284 (1999) 1819.
[7] J.G. Flemming, S.-Y. Lin, Opt. Lett. 24 (1999) 49.
[8] M.C. Wanke, O. Lehmann, K. Muller, Q. Wen, M. Stuke, Science 275 (1997) 1284.
[9] B.H. Cumpston, S.P. Anathavel, S. Barlow, D.L. Dyer, J.E. Ehrlich, L.L. Erskine, A.A. Heikal, S.M. Kuebler, I.Y.S. Lee, D. McCord- Maughon, J.Q. Qin, H. Rockel, M. Rumi, X.L. Wu, S.R. Marder, J.W. Perry, Nature 398 (1999) 51.
[10] Y. Fink, J.N. Winn, S. Fan, C. Chen, J. Michel, J.D. Joannopoulos, E.L. Thomas, Science 282 (1998) 1679.
[11] I.I. Tarhan, G.H. Watson, Phys. Rev. Lett. 76 (1996) 315.
[12] R.D. Pradhan, J.A. Bloodgood, G.H. Watson, Phys. Rev. B 55 (1997) 9503.
[13] A. Imhof, D.J. Pine, Nature 389 (1997) 948.
[14] O.D. Velev, T.A. Jede, R.E. Lobo, A.M. Lenhoff, Nature 389 (1997) 447.
[15] B.T. Holland, C.F. Blanford, A. Stein, Science 281 (1998) 538.
[16] P. Jiang, K.S. Hwang, D.M. Mittleman, J.F. Bertone, V.L. Colvin, J. Am. Chem. Soc. 121 (1999) 11630.
[17] S.H. Park, Y. Xia, Chem. Mater. 10 (1998) 1745.
[18] M. Deutsh, Y.A. Vlasov, D.J. Norris, Adv. Mater. 12 (2000) 1176.
[19] S. Kim, V. Gopalan, Appl. Phys. Lett. 78 (2001) 3015.
[20] Y.-J. Lee, P.V. Braun, Adv. Mater. 15 (2003) 563.
[21] X.L. Xu, G. Friedman, K.D. Humfeld, S.A. Majetich, S.A. Asher, Adv. Mater. 13 (2001) 1681.
[22] J.H. Holtz, S.A. Asher, Nature 389 (1997) 829.
[23] K. Lee, S.A. Asher, J. Am. Chem. Soc. 122 (2000) 9534.
[24] X.L. Xu, G. Friedman, K.D. Humfeld, S.A. Majetich, S.A. Asher, Chem. Mater. 14 (2002) 1249.
[25] S.A. Asher, V.L. Alexeev, A.V. Goponenko, A.C. Sharma, I.K. Lednev, C.S. Wilcox, D.N. Finegold, J. Am. Chem. Soc. 125 (2003) 3322.
[26] S.A. Asher, J. Holtz, L. Liu, Z. Wu, J. Am. Chem. Soc. 116 (1994) 4997.
[27] L. Liu, P. Li, S.A. Asher, J. Am. Chem. Soc. 121 (1999) 4040.
[28] L. Liu, P. Li, S.A. Asher, Nature 397 (1999) 141.
[29] H. Míguez, F. Meseguer, C. López, Á. Blanco, J.S. Moya, J. Requena, A. Mifsud, V. Fornés, Adv. Mater. 10 (1998) 480.
[30] S.H. Foulger, P. Jiang, Y.R. Ying, A.C. Lattam, D.W. Smith Jr., J. Ballato, Adv. Mater. 13 (2001) 1898.